Effective hard-sphere model of diffusion in aqueous polymer solutions

(Stephen S. L. Peppin, Victoria, Canada)

email: speppin@gmail.com

February 11, 2021

Abstract

An effective hard-sphere model of the diffusion and cross-diffusion of salt in unentangled polymer solutions is developed. Given the viscosity, sedimentation coefficient and osmotic pressure of the polymer, the model predicts the diffusion and cross-diffusion coefficients as functions of the polymer concentration and molecular weight. The results are compared with experimental data on NaCl diffusion in aqueous polyethylene glycol solutions, showing good agreement at polymer molecular weights up to $400\,\mathrm{g/L}$. At higher molecular weights the model becomes less accurate, likely because of the effects of entanglement. The tracer Fickian diffusivity can be written in the form of a Stokes-Einstein equation containing the solution viscosity. For NaCl diffusion in polyethylene glycol solutions, the Stokes-Einstein equation breaks down as the polymer size increases. Using Batchelor's viscous correction factor to determine an effective viscosity experienced by the salt ions within the polymer matrix leads to much closer agreement with experiment.

1 Introduction

The diffusion of a dissolved solute in water can be modelled by Fick's law, with a single diffusion coefficient D quantifying the solute flux in response to a concentration gradient [1]. In aqueous polymer solutions the diffusion is more complex, involving cross-diffusion effects between the solute and polymer, and requiring knowledge of a diffusion coefficient matrix for a complete description [1–3]. The diffusion coefficient matrix of salt in polymer solutions has been measured for several systems [4, 5], showing that at high polymer concentrations cross-diffusion effects are significant; in some cases the cross-diffusion coefficients are larger in magnitude than the main Fickian coefficients [6]. In this work a model of cross-diffusion in unentangled, uncharged polymer solutions is obtained by treating the polymers as effective hard spheres. The model uses measurements of the viscosity, osmotic pressure, and sedimentation coefficient of the polymer; given these data explicit expressions for the four diffusion coefficients are obtained as functions of the polymer concentration and molecular weight.

In Section 2 a brief description of cross diffusion in ternary solutions is given; Section 3 reviews Batchelor's hard-sphere cross-diffusion model, and compares the predictions to experimental data on salt diffusion within an aqueous polymer solution. In Section 4 an effective hard-sphere model is developed, that takes account of departures of the polymer molecules from hard-sphere behaviour. Effective hard-sphere radii and viscous mobilities are defined using the osmotic pressure and viscosity of the binary polymer solutions, leading to improved agreement with experiment. Section 5 extends the model to non-dilute polymer concentrations and contains a discussion of the breakdown of the Stokes-Einstein equation in polymer solutions.

2 Cross-diffusion in ternary solutions

The flux equations describing cross-diffusion in ternary solutions can be written in the form

$$\boldsymbol{J}_1 = -D_{11}\boldsymbol{\nabla} n_1 - D_{12}\boldsymbol{\nabla} n_2, \tag{1a}$$

For God so loved the world, that He gave His only begotten Son, that whosoever believeth in Him should not perish, but have everlasting life. John 3:16
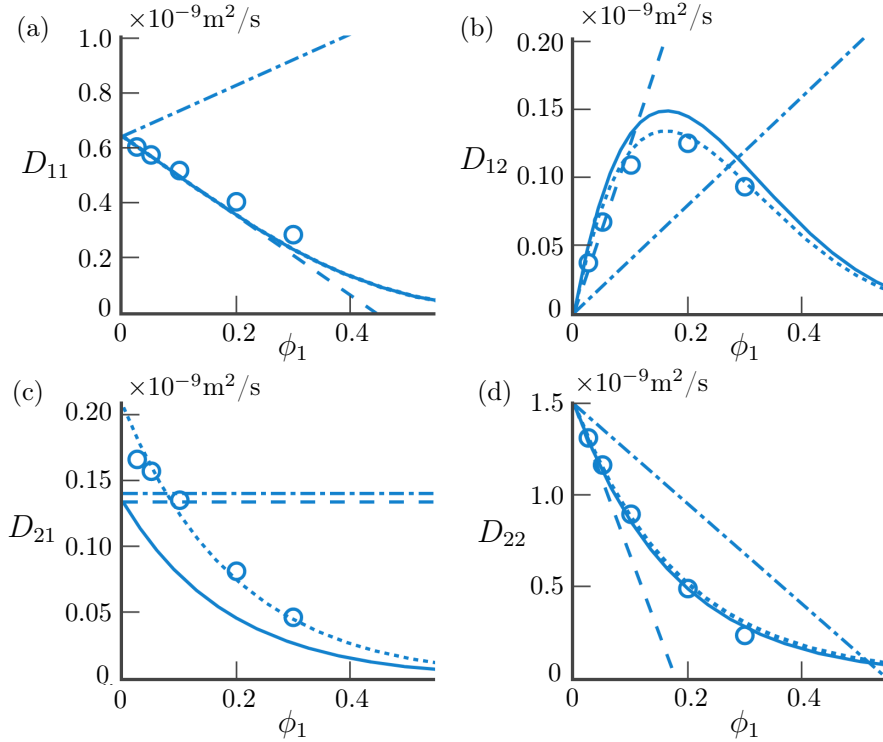
Figure 1: Cross-diffusion coefficients D_{ij} in the ternary solution PEG 200–NaCl–H$_2$O as functions of the PEG hydrodynamic volume fraction ϕ_1. The NaCl concentration is 0.5 M ($\phi_2 = 0.0042$) and the particle size ratio is $\lambda = R_2/R_1 = 0.44$. The data (circles) are from Vergara *et al.* [4]. The dash-dot lines are from the hard-sphere model (10); the dashed lines are from the effective hard-sphere model (19); the solid curves are from the non-dilute effective hard-sphere model (35). The dotted curves are from (35) using the best-fit parameter $\lambda = 0.36$.

$$\boldsymbol{J}_2 = -D_{21}\boldsymbol{\nabla}n_1 - D_{22}\boldsymbol{\nabla}n_2, \tag{1b}$$

where $\boldsymbol{J}_1$ is the flux of the host polymer relative to the volume velocity of the mixture at concentration n_1 (number of polymer molecules per unit volume of mixture), and $\boldsymbol{J}_2$ is the flux of salt at concentration n_2. Here D_{11} is the main Fickian diffusion coefficient of the polymer, while D_{12} is a cross-diffusion coefficient characterizing motion of the host molecules caused by a gradient in salt concentration (*diffusiophoresis*); similarly, D_{22} is the Fickian salt diffusivity, while D_{21} accounts for motion of salt caused by a gradient in the polymer concentration (*osmotic diffusion*) [7].

Figure 1 shows D_{ij} data (circles) obtained by Vergara *et al.* [4] for the diffusion of NaCl within a matrix of polyethylene glycol (PEG) molecules in water. PEG is a hydrophilic, uncharged polymer with many uses in the food, medicine and biotechnology industries, and can be prepared in a range of molecular weights [4]. PEG interacts with other particles in water mainly via excluded volume effects, and is therefore a relatively good system to apply a hard-sphere diffusion model [6]. However, as will be seen in Sections 3.2 and 4.1.2, PEG exhibits significant departures from hard-sphere behaviour even in the dilute limit.

The maximum PEG concentration in the experiments was $C_1 = 3.0\,\text{M} = 3000\,\text{mol/m}^3$, corresponding to a *hydrodynamic* volume fraction $\phi_1 = n_1 v_1 = 0.30$, where $n_1 = Na\,C_1$ is the PEG number density, Na is Avogadro's number, $v_1 = \frac{4}{3}\pi R_1^3$ is the hydrodynamic volume of a PEG molecule and $R_1 = 0.34 \times 10^{-9}\,\text{m}$ is the PEG hydrodynamic radius [8]. Because of the relatively small globular size of the PEG molecules (molecular weight 194 [4]), the polymer molecules were not significantly entangled [9]; however, at these high volume fractions the solution is crowded and

the D_{ij} data is nonlinear, with the polymer diffusiophoresis coefficient D_{12} showing a maximum near $\phi_1 = 0.2$.

The concentration of NaCl in the diffusion experiments was 0.5 M, corresponding to a hydrodynamic volume fraction $\phi_2 = n_2 v_2 = 0.0042$, where $n_2 = N_a C_2$ is the NaCl number density, $v_2 = \frac{4}{3}\pi R_2^3$ and $R_2 = 0.15$ nm is the NaCl hydrodynamic radius [10]. The NaCl main Fickian diffusion coefficient D_{22} in figure 1d decreases rapidly as the PEG concentration increases, reflecting the obstruction effect of the PEG molecules on the diffusion of salt. The relatively large measured values of the cross coefficients D_{12} and D_{21} indicate the importance of cross-diffusion on the motion of NaCl in this system [4].

3 Batchelor's cross-diffusion model

In this section Batchelor's [3] theory of tracer cross-diffusion in hard-sphere suspensions is briefly reviewed and applied to the PEG diffusion data. From nonequilibrium thermodynamics [11, 12] the four diffusion coefficients in a ternary solution can be written in the form

$$D_{ij} = \sum_{k=1}^{2} L_{ik}\mu_{kj} \qquad (i, j = 1, 2), \tag{2}$$

where $L_{ij} = L_{ji}$ are Onsager phenomenological coefficients, μ_i are the reduced chemical potentials per particle and $\mu_{ij} = (\partial\mu_i/\partial n_j)_{T,P,n_{k\neq j}} = \mu_{ji}$ [3, 11–13]. In the following the temperature T and mixture pressure P are assumed constant. In the McMillan-Mayer theory of suspensions the reduced chemical potentials are equal to the chemical potentials of a binary hard-sphere gas, and their derivatives can be written in the dilute limit as

$$\mu_{ij} = k_B T \left(\frac{\delta_{ij}}{n_i} + 2B_{ij} \right) \qquad (i, j = 1, 2), \tag{3}$$

where k_B is Boltzmann's constant, δ_{ij} is the delta function and B_{ij} are the osmotic virial coefficients accounting for interparticle forces [12, 14]. To first order in the volume fractions $\phi_i = v_i n_i$, the phenomenological coefficients L_{ij} in a hard-sphere suspension are

$$L_{ij} = \frac{n_i}{6\pi\eta_0 R_i} \left[\delta_{ij}\left(1 + \sum_{k=1}^{2} K'_{ik}\phi_k\right) + \lambda_{ij}^{-3}K''_{ij}\phi_j \right] \qquad (i, j = 1, 2), \tag{4}$$

where η_0 is the solvent viscosity and K'_{ij} and K''_{ij} are mobility coefficients accounting for viscous interactions between the particles; for hard spheres the mobility coefficients are functions of the particle size ratio $\lambda_{ij} = R_j/R_i$ [3, 13]. In general the mobility coefficients K'_{ij} and K''_{ij} obey the relations

$$\lim_{\lambda_{21}\to 0} K'_{21} = -k_\eta \quad \text{and} \quad K'_{11} + K''_{11} = -k_s, \tag{5a,b}$$

where k_η is the viscosity concentration coefficient and k_s is the sedimentation concentration coefficient, described in more detail in Section 4.1. For hard spheres $k_\eta = 2.5$ and $k_s = 6.55$ [3]. Equation $(5a)$ ensures that when the tracer particles are much larger than the host particles, the effect of the host matrix is to increase the effective viscosity of the fluid by the factor $1 + k_\eta\phi_1$. Similarly, $(5b)$ ensures that when the particles are all the same size ($\lambda_{ij} = 1$), the sedimentation coefficient of the particles is the same as for a monodisperse system with total volume fraction $\phi = \phi_1 + \phi_2$, and is smaller than the sedimentation coefficient of a single particle by the factor $1 - k_s\phi$ [3].

Combining equations (2), (3) and (4) in the dilute tracer limit $\phi_2 \ll \phi_1 \ll 1$ gives, upon neglecting terms of order ϕ_i^2,

$$D_{11} = D_1^0(1 + [b_{11} + K'_{11} + K''_{11}]\phi_1), \qquad D_{12} = D_1^0(b_{12} + K''_{12})\phi_1, \tag{6a,b}$$

$$D_{21} = D_2^0(b_{21} + K''_{21})\phi_2, \qquad D_{22} = D_2^0(1 + K'_{21}\phi_1), \tag{6c,d}$$

where $D_i^0 = k_B T/(6\pi R_i \eta_0)$ is the Stokes-Einstein diffusivity of component i in the pure solvent and $b_{ij} = 2B_{ij}/v_i$ [3, 15].

3.1 Hard-sphere virial coefficients and viscous mobilities

For hard-sphere particles the virial coefficients depend only on the particle radii and are given by the expression [12]

$$B_{ij} = \frac{2}{3}\pi(R_i + R_j)^3, \tag{7}$$

so that

$$b_{ij} = \frac{2B_{ij}}{v_i} = (1 + \lambda_{ij})^3. \tag{8}$$

Batchelor [3] obtained the following approximate expressions for the mobility coefficients of hard-sphere suspensions

$$K'_{ij} = -\frac{2.5}{(1 + b\lambda_{ij})} \quad \text{and} \quad K''_{ij} = \frac{\lambda_{ij}^2}{(1 + \lambda_{ij}^3)} - (\lambda_{ij}^2 + 3\lambda_{ij} + 1), \tag{9a,b}$$

where b is a constant. In the Corrigendum to [3], Batchelor showed that the value $b = 0.16$ ensures agreement of $(9a)$ with the results of numerical simulations to within 5% at all λ_{ij}.

3.2 Hard-sphere results

With (8) and (9), equations (6) can be written in the form

$$D_{11} = D_1^0(1 + 1.45\phi_1), \qquad D_{12} = D_1^0\left(\lambda^3 + 2\lambda^2 + \frac{\lambda^2}{1 + \lambda^3}\right)\phi_1, \tag{10a,b}$$

$$D_{21} = D_2^0\left(\lambda^{-3} + 2\lambda^{-2} + \frac{\lambda^{-2}}{1 + \lambda^{-3}}\right)\phi_2, \qquad D_{22} = D_2^0\left(1 - \frac{2.5}{1 + 0.16/\lambda}\phi_1\right), \tag{10c,d}$$

where $\lambda = \lambda_{12} = R_2/R_1$. Actually, inserting (8) and (9) into $(6a)$ gives $D_{11} = D_1^0(1 + 1.34\phi_1)$, rather than the more exact result $(10a)$. The relatively small difference is caused by the approximate nature of equations (9) [3, 15].

The Stokes-Einstein diffusivity of PEG 200 in water at $25\,^\circ$C is $D_1^0 = 0.64 \times 10^{-9}\,\mathrm{m^2/s}$, and the hydrodynamic radius is $R_1 = k_B T/(6\pi\eta_0 D_1^0) = 0.34\,\mathrm{nm}$ [4]. For NaCl, $D_2^0 = 1.50 \times 10^{-9}\,\mathrm{m^2/s}$ giving a hydrodynamic radius of $R_2 = 0.15\,\mathrm{nm}$ [10], and therefore $\lambda = R_2/R_1 = 0.44$ for PEG 200. With this value for λ, the dash-dot lines in figure 1 show the diffusion coefficients calculated from (10). The hard-sphere model does not agree very well with the D_{ij} data, suggesting that although PEG molecules are relatively globular and inert, they do not behave like hard spheres in aqueous solution. In the next section this is confirmed using osmotic pressure and viscosity data, and a more general model is developed that takes into account the unique hydrodynamic and thermodynamic properties of the PEG molecules.

4 Effective hard-sphere model

In many polymer and colloidal solutions an effective hard-sphere radius R_1^e can be used in place of the hydrodynamic radius R_1, leading to improved agreement between experiment and hard-sphere models [16–18]. In this section a similar effective hard-sphere approach is developed in which osmotic pressure and viscosity data are used to define an effective particle radius and effective viscous mobility coefficients. In order to properly define these quantities a brief discussion of viscosity, diffusion, sedimentation and osmotic pressure in polymer solutions is given below.

4.1 Hydrodynamic coefficients in polymer solutions

To first order in concentration the viscosity η, mutual diffusion coefficient D, sedimentation coefficient s and osmotic pressure Π of a binary polymer-solvent solution can be written as

$$\eta = \eta_0(1 + k_\eta\phi_1), \qquad D = D_0(1 + k_D\phi_1), \tag{11a,b}$$
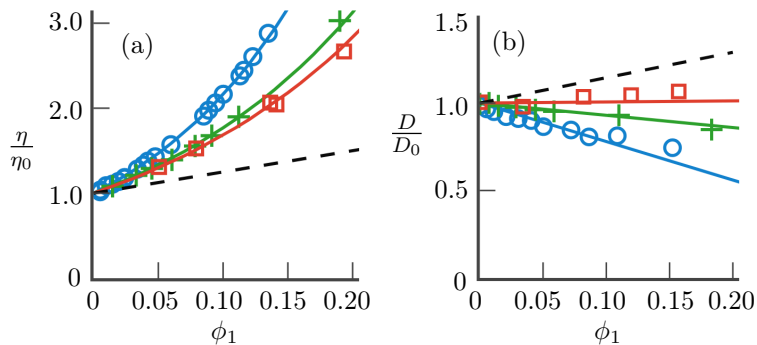
Figure 2: (a) Relative viscosity $\eta(\phi_1)/\eta_0$ of PEG-H$_2$O solutions measured at $25\,^\circ$C by Albright *et al.* [23] (PEG 200, circles; PEG 2000, squares) and by Vergara *et al.* [6] (PEG 400, crosses). The curves are from equation (15) giving the viscosity concentration coefficient k_η values in Table 1. The dashed line is from equation (11a) using the hard-sphere value $k_\eta = 2.5$. (b) PEG-H$_2$O mutual diffusion coefficient $D(\phi_1)$ measured at $25\,^\circ$C by Vergara *et al.* [8] (PEG 200, circles; PEG 400, crosses; PEG 2000, squares). The solid lines are from equations (11b) and (13a) using the coefficient values in Table 1, while the dashed line is the hard-sphere case with $k_D = 1.45$.

$$s = s_0(1 - k_s\phi_1), \qquad \Pi = \Pi_0(1 + k_\Pi\phi_1). \tag{11c,d}$$

In (11a) η_0 is the solvent viscosity and k_η is the viscosity concentration coefficient; in (11b) $D_0 = k_BT/(6\pi R_1\eta_0)$ is the Stokes-Einstein diffusivity of a polymer molecule in the pure fluid solvent and k_D is the diffusion concentration coefficient. Similarly, in (11c) s_0 is the dilute-limit polymer sedimentation coefficient and k_s is the sedimentation concentration coefficient; and in (11d) $\Pi_0 = n_1 k_BT$ is the dilute-limit polymer osmotic pressure and $k_\Pi = B_{11}/v_1 = b_{11}/2$ is the osmotic concentration coefficient, where B_{11} is the second virial coefficient [19–21]. For hard-sphere particles the concentration coefficients in (11) have the known values

$$k_\eta = 2.5, \quad k_\Pi = 4, \quad k_s = 6.55 \quad \text{and} \quad k_D = 1.45, \tag{12}$$

independent of the particle size [19, 21]. For polymers, the values of k_D, k_η, k_Π and k_s often depart from (12) and typically depend on the molecular weight M_1 [8].

The concentration coefficients in (11) are not all independent but are related by the equations

$$k_D = 2k_\Pi - k_s \qquad \text{and} \qquad k_s = \mathcal{R}k_\eta, \tag{13a,b}$$

Equation (13a) is a consequence of the generalized Stokes-Einstein equation [19–21], while (13b) is the Wales-van Holde relation, where $\mathcal{R}$ is the Wales-van Holde ratio [20, 22].

4.1.1 Effective hard-sphere radius

The polymer effective (osmotic) volume is defined as $v_1^e \equiv v_1(k_\Pi/4) = B_{11}/4$ [17, 21] so that the effective hard-sphere radius is

$$R_1^e = R_1 \left(\frac{k_\Pi}{4} \right)^{1/3}. \tag{14}$$

With equation (14) the effective radius can be determined given the osmotic concentration coefficient k_Π. For true hard-sphere particles $k_\Pi = 4$ and $R_1^e = R_1$.

4.1.2 Application to polyethylene glycol

Table 1 gives the Stokes-Einstein diffusivity D_1^0, hydrodynamic radius R_1 and concentration coefficients of PEG in water for three molecular weights [8]. The viscosity coefficient k_η values in

	$D_1^0\,(\times 10^{-9}\mathrm{m^2/s})$	R_1 (nm)	k_Π	k_η	k_s	R_1^e (nm)	λ
PEG 200	0.64	0.34	1.81	7.7	5.8	0.26	0.44
PEG 400	0.44	0.49	1.85	5.7	4.3	0.38	0.30
PEG 2000	0.20	1.16	1.98	5.2	3.9	0.85	0.13

Table 1: Physical parameters for PEG-H$_2$O solutions at 25 °C.

	$D_2^0\,(\times 10^{-9}\mathrm{m^2/s})$	R_2 (nm)	i_H
NaCl	1.5	0.15	1.8

Table 2: Physical parameters for 0.5 M NaCl-H$_2$O solutions at 25 °C.

Table 1 have been determined from figure 2a, which shows measurements of the viscosity η of PEG-H$_2$O solutions as a function of ϕ_1. To extract the viscosity concentration coefficient k_η, the data in figure 2 has been fit to the exponential equation [24, 25]

$$\eta = \eta_0 \mathrm{e}^{k_\eta \phi_1}, \tag{15}$$

which reduces to (11b) in the dilute limit. The PEG viscosity coefficient is significantly larger than the hard-sphere value of 2.5 at all molecular weights. This is a consequence of the hydrated, globular nature of the PEG molecules, which tend to interact with each other more strongly in a shear flow than would occur for true hard-spheres [24].

The osmotic concentration coefficients k_Π in Table 1 have been obtained from measurements of the second virial coefficient by Yasukawa *et al.* [26] (Appendix A). The osmotic concentration coefficient is smaller than the hard-sphere value $k_\Pi = 4$. The effective PEG radius can be calculated from equation (14) as $R_1^e = R_1(k_\Pi/4)^{1/3}$, giving the values shown in Table 1. The effective osmotic radius of PEG is smaller than its hydrodynamic radius. The relatively large hydrodynamic radius R_1 reflects the hydrophilic nature of PEG molecules, which tend to adsorb water molecules within the polymer coils and drag the adsorbed water along during motion [9].

The sedimentation concentration coefficient k_s has been measured for many polymers [27] but is not yet available for PEG. Given k_η, however, the sedimentation concentration coefficient can be estimated from equation (13b) as $k_s = \mathcal{R}k_\eta$. For hard spheres the Wales-van Holde ratio is $\mathcal{R} = 6.55/2.5 = 2.62$, while for polymers and macromolecules $\mathcal{R}$ typically varies between 0.2 for rod-like molecules and 1.6 for globular particles [28]. Low molecular weight PEG acts like an ideal polymer [29], in which case $\mathcal{R} = 0.75$ [30]; using this value for $\mathcal{R}$ gives the k_s values shown in Table 1.

Given k_s, the diffusion concentration coefficient k_D can be obtained from equation (13a) as $k_D = 2k_\Pi - k_s$. Figure 2b shows $D(\phi_1)$ calculated from equation (11b) with (13a) (solid lines), along with experimental PEG-H$_2$O mutual diffusion coefficient data from Vergara *et al.* [8], showing good agreement. The dashed line in figure 2b shows the hard-sphere case ($k_D = 1.45$); as with the viscosity and osmotic pressure the PEG diffusion coefficient shows significant departures from hard-sphere behaviour, and the difference depends on the polymer molecular weight.

4.1.3 NaCl

The hydrodynamic radius R_2 of NaCl at 25 °C is 0.15 nm and the Stokes-Einstein diffusivity in water is $D_2^0 = 1.5 \times 10^{-9}\,\mathrm{m^2/s}$ [4, 10] (Table 2). Here it is assumed that the NaCl osmotic radius is approximately equal to the hydrodynamic radius, $R_2^e \approx R_2$. Also shown in Table 2 is the NaCl van't Hoff coefficient i_H evaluated at $C_2 = 0.5$ M [31], which will be used in Section 5.

4.2 Effective virial coefficients and viscous mobilities

In the effective hard-sphere model the osmotic virial coefficients (7) become $B_{ij} = \frac{2}{3}\pi(R_i^e + R_j^e)^3$ so that

$$b_{ij} = \frac{2B_{ij}}{v_i} = \left(\frac{R_i^e + R_j^e}{R_i}\right)^3 \tag{16}$$

in place of (8). The hydrodynamic mobilities K'_{ij} and K''_{ij} will also depart from the hard-sphere expressions (9) because of the asphericity, flexibility and hydration of the polymer molecules [32–34]. For relatively globular, unentangled polymers effective mobility coefficients can be defined as

$$K'_{ij} = a' \left(\frac{-2.5}{(1 + 0.16\lambda_{ij})} \right) \quad \text{and} \quad K''_{ij} = a'' \left(\frac{\lambda_{ij}^2}{(1 + \lambda_{ij}^3)} - (\lambda_{ij}^2 + 3\lambda_{ij} + 1) \right), \qquad (17a,b)$$

where the viscous factor a' and asphericity factor a'' can be obtained from the PEG viscosity data. Combining $(17a,b)$ with $(5a,b)$ gives

$$a' = \frac{k_\eta}{2.5} \quad \text{and} \quad a'' = \left(\frac{k_s}{4.5} - \frac{k_\eta}{5.5} \right). \qquad (18a,b)$$

4.3   Effective hard-sphere diffusivities

Using (16)–(18) in (6) and assuming $R_2^e \approx R_2$ gives the following effective hard-sphere expressions for the cross-diffusion coefficients, bearing in mind that $\lambda = \lambda_{12} = \lambda_{21}^{-1}$, $k_\Pi = b_{11}/2$ and $K'_{11} + K''_{11} = -k_s$,

$$D_{11} = D_1^0 [1 + (2k_\Pi - k_s)\phi_1], \qquad (19a)$$

$$D_{12} = D_1^0 \left[\left(\frac{R_1^e}{R_1} + \lambda \right)^3 + a'' \left(\frac{\lambda^2}{1 + \lambda^3} - (\lambda^2 + 3\lambda + 1) \right) \right] \phi_1, \qquad (19b)$$

$$D_{21} = D_2^0 \left[\left(1 + \frac{R_1^e}{R_1}\lambda^{-1} \right)^3 + a'' \left(\frac{\lambda^{-2}}{1 + \lambda^{-3}} - (\lambda^{-2} + 3\lambda^{-1} + 1) \right) \right] \phi_2, \qquad (19c)$$

$$D_{22} = D_2^0 \left(1 - \frac{k_\eta \phi_1}{1 + 0.16/\lambda} \right). \qquad (19d)$$

Equations (19) are plotted as the dashed lines in figure 1, using the k_Π, k_η and k_s values given in Table 1, showing better agreement with the experimental data. However, the model does not capture the ϕ_1 dependence of the NaCl osmotic-diffusion coefficient D_{21}, nor the nonlinearities in the data at higher PEG concentrations. To account for these effects in the next section a non-dilute effective hard-sphere model is developed.

5   Concentrated solutions

For tracer diffusion in concentrated solutions the diffusivities D_{ij} can be written in the form

$$D_{11} = n_1 \frac{k}{\eta_0} \Pi_1, \qquad D_{12} = n_1 \frac{k}{\eta_0} \sigma \pi_2, \qquad (20a,b)$$

$$D_{21} = \frac{n_2}{n_1} \ell D_{11} - \gamma D_t, \quad D_{22} = D_t, \qquad (20c,d)$$

where k is the permeability and Π the osmotic pressure of the host-particle matrix, π is the osmotic pressure of the tracer particles in the pores of the matrix, $\Pi_i = (\partial \Pi / \partial n_i)_{T,P,n_j}$ and $\pi_i = (\partial \pi / \partial n_i)_{T,P,n_j}$ are derivatives of the osmotic pressure with respect to concentration, $\gamma = -\pi_1/\pi_2$ is the host/tracer preferential interaction coefficient, σ is the reflection coefficient of the host matrix, D_t is the tracer diffusivity within the pore space, $\ell = (\sigma + \alpha - 1)/\alpha$ is a cross-diffusion factor and α is the equilibrium partition coefficient of the tracer between the pore space and bulk solvent [15].

5.1 Osmotic pressure

The osmotic pressure of the host-particle matrix can be written as

$$\Pi = n_1 k_B T Z, \tag{21}$$

where Z is the compressibility factor (osmotic coefficient). Assuming the NaCl concentration is sufficiently low that it does not significantly affect the uncharged polymer osmotic pressure (*i.e.* assuming $\Pi_2 = 0$), in the effective hard-sphere model Z is given at volume fractions up to 0.55 by the Carnahan-Starling equation

$$Z = \frac{1 + \phi_1^e + \phi_1^{e2} - \phi_1^{e3}}{(1 - \phi_1^e)^3}, \tag{22}$$

where $\phi_1^e = v_1^e n_1 = \phi_1 k_\Pi / 4$ is the effective (osmotic) volume fraction and v_1^e is the PEG effective volume defined in Section 4.1.1 [17, 35]. Differentiating (21) with respect to n_1 gives, bearing in mind that v_1^e is a constant,

$$\Pi_1 = \left(\frac{\partial n_1 k_B T Z}{\partial n_1}\right)_{T,P,n_2} = k_B T \left(\frac{\mathrm{d}\phi_1^e Z}{\mathrm{d}\phi_1^e}\right) = k_B T \left[\frac{1 + 4\phi_1^e + 4\phi_1^{e\,2} - 4\phi_1^{e\,3} + \phi_1^{e\,4}}{(1 - \phi_1^e)^4}\right]. \tag{23}$$

The salt osmotic pressure in the pore fluid is

$$\pi = i n_r k_B T, \tag{24}$$

where i is the van't Hoff factor, $n_r = n_2/\alpha$ is the salt concentration in the pore space and α is the salt partition coefficient between the pores and the bulk fluid [15, 36],

$$\alpha = \mathrm{e}^{-b_{12}\phi_1}. \tag{25}$$

Here b_{12} is given by equation (16) as $b_{12} = 2B_{12}/v_1 = (R_1^e/R_1 + \lambda)^3$, assuming as in Section 4.3 that $R_2^e = R_2$. For NaCl in the infinitely dilute limit the Na$^+$ and Cl$^-$ ions completely dissociate and $i = 2$; at higher concentrations i is less than 2 (partial dissociation), and at $C_2 = 0.5\,\mathrm{M}$ $i = 1.8$ [31].

Differentiating (24) with respect to n_i gives

$$\pi_1 = i k_B T n_2 b_{12} v_1/\alpha \qquad \text{and} \qquad \pi_2 = i k_B T/\alpha, \tag{26a,b}$$

from which the preferential interaction coefficient γ can be obtained as

$$\gamma = -\pi_1/\pi_2 = -n_2 b_{12} v_1 = -\phi_2 b_{12}/\lambda^3. \tag{27}$$

Equations (25) and (27) account for the fact that the PEG molecules tend to preferentially adsorb water molecules while rejecting the Na$^+$ and Cl$^-$ ions into the pore fluid, so that n_r in the pore space is larger than the bulk salt concentration n_2 [12, 36].

5.2 Permeability

The permeability of the host matrix to the flow of water can be written as

$$k = \frac{f}{6\pi R_1 n_1}, \tag{28}$$

where $f = s/s_0$ is the dimensionless sedimentation coefficient (friction coefficient), given by (11c) in the dilute limit [16, 37]. Here it is assumed that for relatively globular polymer molecules f is given by a hard-sphere Richardson-Zaki equation [16, 38]

$$f = (1 - \phi_1)^{k_s}, \tag{29}$$

where k_s is the sedimentation concentration coefficient obtained in Section 4.1.2. Equation (29) reduces to equation (11c) in the limit $\phi_1 \to 0$.

5.3 Tortuosity and reflection coefficient

The tracer diffusivity D_t can be written in the form

$$D_t = \tau D_2^0, \tag{30}$$

where τ is the diffusive tortuosity factor accounting for the hindrance effect on the tracer particle diffusion within the host matrix [15, 39]. In the dilute limit $\phi_1 \to 0$, comparison of $(20d)$ with $(6d)$ gives

$$\tau = 1 - \tau_1 \phi_1, \tag{31}$$

where $\tau_1 = -K_{21}'$. Similarly, equation $(20b)$ in the limit $\phi_1 \to 0$ becomes $D_{12} = D_1^0 \sigma$, and comparison with $(6b)$ gives

$$\sigma = \sigma_1 \phi_1, \tag{32}$$

where $\sigma_1 = b_{12} + K_{12}''$.

In the hard sphere case, constitutive equations for τ and σ in concentrated suspensions have been obtained by using capillary flow models and a power-law equation for the hard-sphere viscosity [15]. For unentangled polymer solutions the viscosity is more accurately described by exponential functions [24, 25], as demonstrated for PEG in Section 4.1.2. By analogy with equation (15) this suggests constitutive equations of the form

$$\tau = \mathrm{e}^{-\tau_1 \phi_1} \qquad \text{and} \qquad \sigma = 1 - \mathrm{e}^{-\sigma_1 \phi_1}, \tag{33a,b}$$

which reduce to (31) and (32) in the dilute limit.

The tortuosity τ and reflection coefficient σ measure the degree to which the salt ions can diffuse and advect, respectively, through the host polymer matrix. In the dilute limit $\phi_1 \to 0$, $\tau = 1$ and $\sigma = 0$, and there is no hindrance to the diffusion or advection of salt. At higher polymer concentrations $\tau \to 0$ while $\sigma \to 1$, and the motion of salt is significantly hindered relative to the host matrix [15]. Finally, given σ and α the cross-diffusion factor $\ell = (\sigma + \alpha - 1)/\alpha$ in $(20c)$ is

$$\ell = 1 - \mathrm{e}^{-K_{12}'' \phi_1}. \tag{34}$$

The cross-diffusion factor is a measure of the viscous momentum transfer between the tracer and host particles, and is related to the Onsager phenomenological coefficients L_{ij} by the relation $\ell = n_1 L_{12}/(n_2 L_{11})$ [15]. Similarly to σ, $\ell \to 0$ as $\phi_1 \to 0$ while $\ell \to 1$ as $\sigma \to 1$.

5.4 Results

With (21)–(34), the diffusion coefficients in equations (20) take the form

$$D_{11} = D_1^0 (1 - \phi_1)^{k_s} \left[\frac{1 + 4\phi_1^e + 4\phi_1^{e\,2} - 4\phi_1^{e\,3} + \phi_1^{e\,4}}{(1 - \phi_1^e)^4} \right], \tag{35a}$$

$$D_{12} = i D_1^0 (1 - \phi_1)^{k_s} \left(\mathrm{e}^{b_{12}\phi_1} - \mathrm{e}^{-K_{12}''\phi_1} \right), \tag{35b}$$

$$D_{21} = \frac{\phi_2}{\phi_1 \lambda^3} \left[\left(1 - \mathrm{e}^{-K_{12}''\phi_1} \right) D_{11} + \phi_1 b_{12} D_{22} \right], \tag{35c}$$

$$D_{22} = D_2^0 \mathrm{e}^{K_{21}'\phi_1}, \tag{35d}$$

where $\phi_1^e = \phi_1 k_\Pi/4$, $i = 1.8$ and b_{12}, K_{12}'' and K_{21}' are as given in Section 4.2:

$$b_{12} = \left(\frac{R_1^e}{R_1} + \lambda \right)^3, \quad K_{12}'' = \left(\frac{k_s}{4.5} - \frac{k_\eta}{5.5} \right) \left(\frac{\lambda^2}{1 + \lambda^3} - (1 + 3\lambda + \lambda^2) \right) \quad \text{and} \quad K_{21}' = \frac{-k_\eta}{1 + 0.16/\lambda}.$$

The solid blue curves in figure 1 show the D_{ij} calculated from (35) using the coefficient values in Table 1. The model shows good agreement with the data, and reproduces the nonlinear shape of the PEG diffusiophoresis coefficient D_{12}, including the observed maximum at $\phi_1 \approx 0.2$. A closer match to the D_{12} and D_{21} data can be obtained by using a best-fit value $\lambda = 0.36$ for the particle size ratio, as shown by the dotted curves in figure 1.
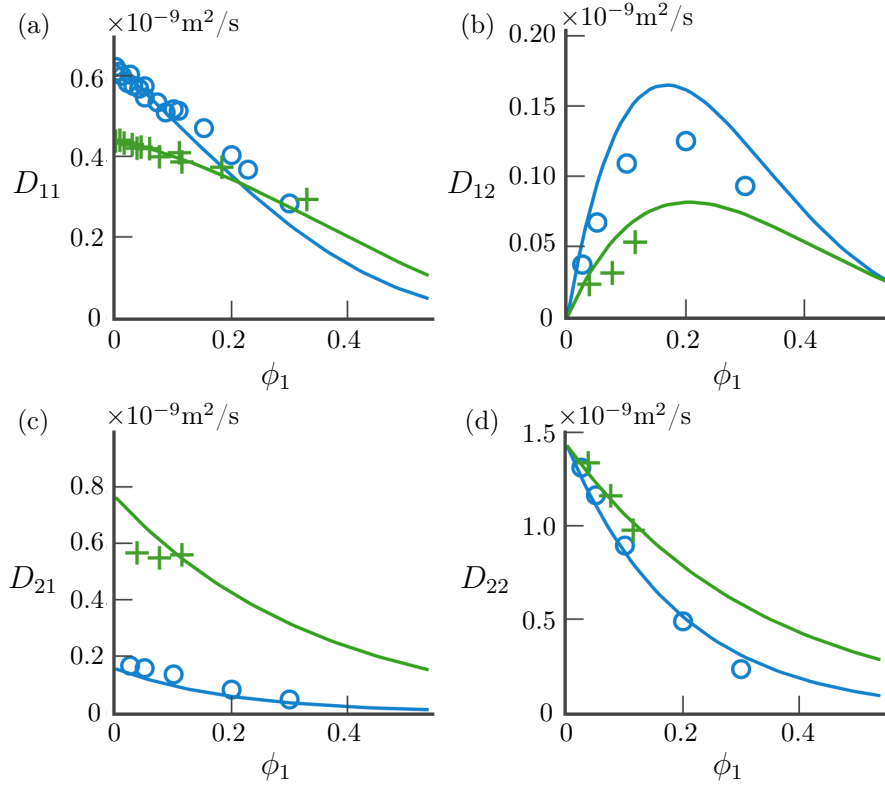
Figure 3: Cross-diffusion coefficients D_{ij} in the system PEG–NaCl–H$_2$O. The data are from Vergara *et al.* [4] (PEG 200, 0.5 M NaCl, circles) and Vergara *et al.* [6] (PEG 400, 0.78 M NaCl, crosses). Also included in (a) is mutual diffusion coefficient data from Vergara *et al.* [8]. The solid curves are from (35) with the coefficient values in Table 1.

5.4.1 Molecular weight dependence

As a further test of the model, figure 3 shows the effect on the D_{ij} of increasing the NaCl concentration to 0.78 M ($\phi_2 = 0.0066$) and increasing the molecular weight of the polymer molecules to PEG 400. The plus symbols are data from the experiments of Vergara *et al.* [6]. The solid green curves are from equation (35) using the coefficients for PEG 400 in Table 1. The model captures the concentration dependence of D_{11} and D_{22} quite well for PEG 400, while slightly over-predicting the PEG diffusiophoresis coefficient D_{12} and the NaCl osmotic-diffusion coefficient D_{21} at low concentrations.

At low PEG concentrations ($\phi_1 \to 0$) equation (35c) becomes

$$D_{21} = \frac{\phi_2}{\lambda^3}\left[K''_{12}D_{11} + b_{12}D_{22}\right] \approx \phi_2 \frac{b_{12}}{\lambda^3}D_{22},$$

which is similar to expressions for D_{21} obtained by Vergara *et al.* [6] and Annunziata [5], which also predict that D_{21} is proportional to D_{22} in the dilute polymer limit. Since D_{22} decreases with ϕ_1, the models all predict that D_{21} decreases with increasing PEG concentration. The D_{21} data for PEG 400 appears to be independent of ϕ_1, in contrast to the models and the PEG 200 data. The measurements of the osmotic diffusion coefficient D_{21} tend to have more experimental uncertainty than the other coefficients [4, 6]. Further support for a decrease in D_{21} comes from experiments on the system PEG 2000–NaCl–H$_2$O [5], which also also show D_{21} decreasing as the polymer concentration is increased.

The model predictions for PEG 2000 solutions (not shown) are qualitatively similar but not as accurate as for the smaller molecular weights. This may reflect a breakdown of the effective

hard-sphere model – PEG 2000 molecules are much less spherical in solution than PEG 200 [32], and the PEG 2000 particles are entangled at relatively low concentrations [9]. Both of these effects negate the assumptions of the effective hard-sphere model developed here. Nevertheless, the results in figure 3 suggest the model is able to predict with a fair degree of accuracy the diffusion coefficients in low-molecular weight PEG solutions as functions of both concentration and polymer size.

5.4.2 Breakdown of the Stokes-Einstein equation

For large tracer particles with $\lambda \gg 1$, the Fickian diffusivity D_{22} can be written in the form of a Stokes-Einstein equation

$$D_{22} = \frac{k_B T}{6\pi\eta R_2}, \qquad (36)$$

where η is the viscosity of the polymer solution [40, 41]. Equation (36) is valid as $\lambda \to \infty$ because for large tracer particles the polymer solution behaves like an effective continuum. For small tracer particles with $\lambda < 1$, however, the tracer particles are significantly affected by the molecular nature of the polymer molecules and the Stokes-Einstein relation (36) breaks down [42–44]. Physically, the tracer particles experience a reduced effective viscosity η_e within the pore space that is smaller than the macroscopic viscosity η [15, 45, 46]. Figure 4 shows D_{22} calculated from (36) with equation (15) for the PEG viscosity (dotted curves), along with experimental data for three polymer molecular weights (PEG 200, $\lambda = 0.44$; PEG 400, $\lambda = 0.30$; and PEG 2000, $\lambda = 0.13$). The Stokes-Einstein relation (36) tends to underestimate the NaCl diffusivity, and the discrepancy becomes larger as λ decreases.

In order to account for pore-scale viscosity effects the tracer diffusivity can be written in the form of an effective Stokes-Einstein equation

$$D_{22} = \frac{k_B T}{6\pi\eta_e R_2}, \qquad (37)$$

where η_e is the effective viscosity experienced by the tracer particles within the pore space [15, 47]. Comparing (37) with (35d) gives an expression for the effective viscosity

$$\eta_e = \eta_0 \exp\left[\frac{k_\eta \phi_1}{(1 + 0.16/\lambda)}\right], \qquad (38)$$

which reduces to (15) as $\lambda \to \infty$. Equation (38) contains Batchelor's viscous correction factor $(1 + 0.16/\lambda)$ [3]. When $\lambda \to \infty$ (large tracer particles or small host particles), this factor is equal to 1 and the effective viscosity η_e is equal to the solution viscosity η. For very small tracer particles relative to the host molecules ($\lambda \to 0$) the viscous factor becomes large and η_e approaches the solvent viscosity η_0. The solid curves in figure 4 are from equations (37) and (38), showing much better agreement with experiment. This suggests that the breakdown of the Stokes-Einstein equation for NaCl diffusion in low molecular weight PEG solutions is caused mainly by long-range hydrodynamic interactions between the salt ions and the polymer matrix [48].

5.5   Discussion

The effective hard-sphere model developed here relies on hydrodynamic results obtained for impermeable spherical particles with no-slip boundary conditions [3]. The mobility coefficients have been modified using viscosity data leading to good results for relatively low molecular weight PEG solutions, but likely limit the model to systems in which the polymers are unentangled and roughly spherical in shape. A more general model of the hydrodynamics for polymer molecules may be porous particles with slip or partial slip boundary conditions [50] or dumbell chain models [51, 52]; however, expressions for K'_{ij} and K''_{ij} for these cases are not at present available. Equations (20) may still apply even in solutions of entangled or charged macromolecules given appropriate expressions for the thermodynamic and transport coefficients. For example, Cohen *et al.* [53] have
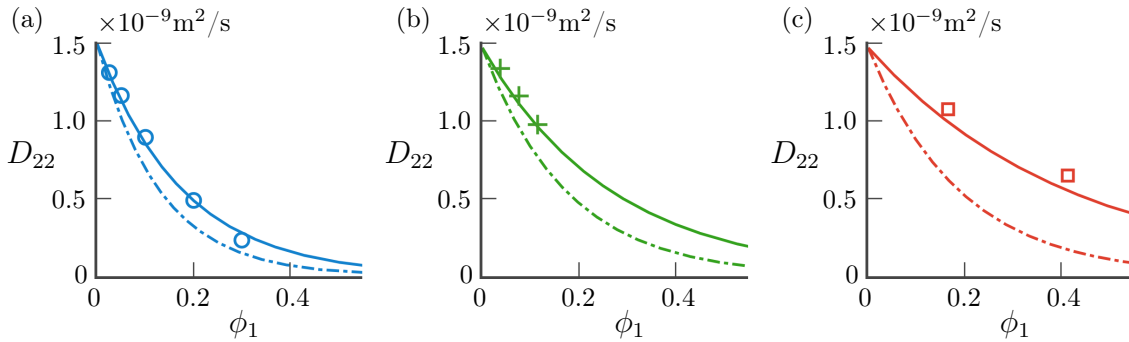
Figure 4: NaCl main diffusion coefficient D_{22} in the system PEG–NaCl–H$_2$O. The data were obtained using three molecular weights: (a) PEG 200 (circles) [4]; (b) PEG 400 (crosses) [6]; and (c) PEG 2000 (squares) [49]. The dash-dot curves are from the Stokes-Einstein equation (36) and the solid curves are from equation (37).

shown that a des Cloizeaux osmotic pressure of the form $\Pi = C_1 RT[1 + \alpha_C\,(C_1/C_1^*)^{5/4}]$ gives good agreement with experimental data in entangled PEG solutions, where α_C is a coefficient that depends on the molecular weight [54]. Similarly, Ullmann *et al.* [48], Holyst *et al.* [44] and Kohli and Mukhopadhyay [55] have shown that the tracer diffusivity and viscosity of entangled PEG solutions can be modelled via stretched exponential functions of the form $D_{22} = D_2^0 \exp(-\beta\phi_1^\nu)$ and $\eta = \eta_0 \exp(a\phi_1^b)$, where β, ν, a and b are constants. An extension of the present model to entangled solutions could potentially be developed using these and similar expressions for the coefficients σ, α and f, and will be explored in future work.

6   Conclusion

An effective hard-sphere model of salt diffusion in uncharged, unentangled hydropolymer solutions has been developed. Given the viscosity, sedimentation coefficient and osmotic pressure of the polymer, the model predicts the ternary diffusion coefficients as functions of polymer size and concentration. The model uses hydrodynamic results obtained for hard spherical particles, modified using the viscosity and osmotic pressure of the polymer. This leads to good results for NaCl diffusion in low molecular weight polyethylene glycol solutions. It is anticipated the model will apply more generally to crowded solutions in which the host molecules are inert, unentangled and roughly spherical in shape.

Acknowledgements

A   Osmotic virial coefficients

Depending on the concentration variable used, the dilute-limit osmotic pressure of a binary solution, equation (11d), is given in the literature in several equivalent forms, including

$$\begin{aligned}
\Pi &= n_1 k_B T(1 + B_{11}n_1)\\
&= n_1 k_B T(1 + k_\Pi \phi_1)\\
&= C_1 RT(1 + B_{11}^* C_1)\\
&= \rho_1 RT(1/M_1 + A_{11}\rho_1),
\end{aligned} \tag{39}$$

where $C_1 = n_1/Na$ is the molar concentration (mol/L), $\rho_1 = M_1 C_1 = M_1 n_1/Na$ is the mass concentration (g/L), $R = k_B Na$ is the gas constant and Na is Avogadro's constant. Here B_{11} is the second virial coefficient, B_{11}^* is the mole-based second virial coefficient (L/mol) and A_{11} is the mass based second virial coefficient (mol L/g^2). They are related to each other by the equations $B_{11}^* = B_{11} Na = k_\Pi v_1 Na = M_1^2 A_{11}$.

Yasukawa *et al.* [26] measured A_{11} for several PEG molecular weights at $T = 298\,\mathrm{K}$ and obtained $RTA_{11} = 1.11 \times 10^{-4}\,\mathrm{bar\,L^2/g^2}$ for PEG 200, where $R = 0.08314\,\mathrm{L\,bar/K/mol}$ is the universal gas constant, giving $A_{11} = 4.48 \times 10^{-9}\,\mathrm{mol\,m^3/g^2}$ and $k_\Pi = M_1^2 A_{11}/(Na\,v_1) = 1.81$. Gaube *et al.* [56] also measured A_{11} for PEG 200, at a slightly lower temperature of 293 K, and obtained a larger value $A_{11} = 7.16 \times 10^{-9}\,\mathrm{mol\,m^3/g^2}$, giving $k_\Pi = 2.92$. Here the data of Yasukawa *et al.* [26] has been used, as the experiments were conducted at the same temperature as the PEG cross-diffusion experiments [4].

For PEG 600 Yasukawa *et al.* [26] obtained $RTA_{11} = 5.86 \times 10^{-5}\,\mathrm{bar\,L^2/g^2}$; extrapolation between the PEG 200 and PEG 600 values gives $RTA_{11} \approx 8.48 \times 10^{-5}\,\mathrm{bar\,L^2/g^2}$ for PEG 400, yielding $k_\Pi = 1.85$. Finally, for PEG 2000 $RTA_{11} = 4.00 \times 10^{-5}\,\mathrm{bar\,L^2/g^2}$ [26] giving $k_\Pi = 1.98$.

References

[1] E. L. Cussler. *Diffusion: Mass Transfer in Fluid Systems.* Cambridge University Press, U.K., 2009.

[2] J. S. Kirkaldy. Diffusion in multicomponent metallic systems. *Canadian Journal of Physics*, **35**, 435–440, 1957.

[3] G. K. Batchelor. Diffusion in a dilute polydisperse system of interacting spheres. *Journal of Fluid Mechanics*, **131**, 155–175, 1983; and Corrigendum **137**, 467–469, 1983.

[4] A. Vergara, O. Annunziata, L. Paduano, D. G. Miller, J. G. Albright, and R. Sartorio. Multicomponent Diffusion in Crowded Solutions. 2. Mutual Diffusion in the Ternary System tetra(ethylene glycol)–NaCl–water. *The Journal of Physical Chemistry B*, **108**, 2764–2772, 2004.

[5] O. Annunziata, A. Vergara, L. Paduano, R. Sartorio, D. G. Miller, and J. G. Albright. Quaternary diffusion coefficients in a protein-polymer-salt-water system determined by Rayleigh interferometry. *The Journal of Physical Chemistry B*, **113**, 13446–13453, 2009.

[6] A. Vergara, L. Paduano, V. Vitagliano, and R. Sartorio. Multicomponent diffusion in crowded solutions. 1. Mutual diffusion in the ternary system poly(ethylene glycol)400–NaCl–water. *Macromolecules*, **34**, 991–1000, 2001.

[7] O. Annunziata, D. Buzatu, and J. G. Albright. Protein diffusiophoresis and salt osmotic diffusion in aqueous solutions. *The Journal of Physical Chemistry B*, **116**, 12694–12705, 2012.

[8] A. Vergara, L. Paduano, V. Vitagliano, and R. Sartorio. Mutual diffusion in aqueous solution of poly(ethylene glycol) samples. Some comments on the effect of chain length and polydispersity. *Phys. Chem. Chem. Phys.*, **1**, 5377–5383, 1999.

[9] A. Vergara, L. Paduano, G. D'Errico, and R. Sartorio. Network formation in polyethylene glycol solutions. An intradiffusion study. *Phys. Chem. Chem. Phys.*, **1**, 4875–4879, 1999.

[10] V. Vitagliano and P. A. Lyons. Diffusion coefficients for aqueous solutions of sodium chloride and barium chloride. *Journal of the American Chemical Society*, **78**, 1549–1552, 1956.

[11] S. R. deGroot and P. Mazur. *Non-Equilibrium Thermodynamics.* North-Holland Publishing Co., Amsterdam, 1962.

[12] O. Annunziata. On the role of solute solvation and excluded-volume interactions in coupled diffusion. *The Journal of Physical Chemistry B*, **112**, 11968–11975, 2008.

[13] G. K. Batchelor. Note on the Onsager symmetry of the kinetic coefficients for sedimentation and diffusion in a dilute bidispersion. *Journal of Fluid Mechanics*, **171**, 509–517, 1986.

[14] A. Santos and R. D. Rohrmann. Chemical-potential route for multicomponent fluids. *Phys. Rev. E*, **87**, 052138, 2013.

[15] S. S. L. Peppin. Theory of tracer diffusion in concentrated hard-sphere suspensions. *J. Fluid Mech.*, **870**, 1105–1126, 2019.

[16] W. B. Russel, D. A. Seville, and W. R. Schowalter. *Colloidal Dispersions*. Cambridge University Press, U.K., 1989.

[17] A. P. Minton. The effective hard particle model provides a simple, robust, and broadly applicable description of nonideal behavior in concentrated solutions of bovine serum albumin and other nonassociating proteins. *Journal of Pharmaceutical Sciences*, **96**, 3466–3469, 2007.

[18] Zhe Wang, Antonio Faraone, Panchao Yin, Lionel Porcar, Yun Liu, Changwoo Do, Kunlun Hong, and Wei-Ren Chen. Dynamic equivalence between soft star polymers and hard spheres. *ACS Macro Letters*, **8**, 1467–1473, 2019.

[19] G. K. Batchelor. Brownian diffusion of particles with hydrodynamic interaction. *Journal of Fluid Mechanics*, **74**, 1–29, 1976.

[20] A. J. Rowe. The concentration dependence of transport processes: A general description applicable to the sedimentation, translational diffusion, and viscosity coefficients of macromolecular solutes. *Biopolymers*, **16**, 2595–2611, 1977.

[21] M. M. Kops-Werkhoven and H. M. Fijnaut. Dynamic light scattering and sedimentation experiments on silica dispersions at finite concentrations. *The Journal of Chemical Physics*, **74**, 1618–1625, 1981.

[22] M. Wales and K. E. Van Holde. The concentration dependence of the sedimentation constants of flexible macromolecules. *Journal of Polymer Science*, **14**, 81–86, 1954.

[23] J. G. Albright, L. Paduano, R. Sartorio, A. Vergara, and V. Vitagliano. Multicomponent diffusion in systems containing molecules of different size. 1. Mutual diffusion in the ternary system poly(ethylene glycol) 2000 + poly(ethylene glycol) 200 + water. *Journal of Chemical & Engineering Data*, **46**, 1283–1291, 2001.

[24] D. K. Thomas and T. A. J. Thomas. Viscosity – concentration relationships in solutions of high polymers. *Journal of Applied Polymer Science*, **3**, 129–131, 1960.

[25] George D. J. Phillies. The hydrodynamic scaling model for polymer self-diffusion. *The Journal of Physical Chemistry*, **93**, 5029–5039, 1989.

[26] Masahiro Yasukawa, Yasuhiro Tanaka, Tomoki Takahashi, Masafumi Shibuya, Shoji Mishima, and Hideto Matsuyama. Effect of molecular weight of draw solute on water permeation in forward osmosis process. *Industrial & Engineering Chemistry Research*, **54**, 8239–8246, 2015.

[27] John J. Correia and Walter F. Stafford. Sedimentation velocity: A classical perspective. In James L. Cole, editor, *Analytical Ultracentrifugation*, volume 562 of *Methods in Enzymology*, pages 49 – 80. Academic Press, 2015.

[28] J.M. Creeth and C.G. Knight. On the estimation of the shape of macromolecules from sedimentation and viscosity measurements. *Biochimica et Biophysica Acta (BBA) - Biophysics including Photosynthesis*, **102**, 549 – 558, 1965.

[29] Hwankyu Lee, Richard M. Venable, Alexander D. MacKerell, and Richard W. Pastor. Molecular dynamics studies of polyethylene oxide and polyethylene glycol: Hydrodynamic radius and shape anisotropy. *Biophysical Journal*, **95**, 1590 – 1599, 2008.

[30] M. Muthukumar. Concentration dependent friction coefficients of polymer molecules in dilute solutions. I. *The Journal of Chemical Physics*, **78**, 2764–2772, 1983.

[31] R. Heyrovská. Physical electrochemistry of strong electrolytes based on partial dissociation and hydration: Quantitative interpretation of the thermodynamic properties of NaCl(aq) from "zero to saturation". *Journal of The Electrochemical Society*, **143**, 1789–1793, 1996.

[32] D. K. Thomas and A. Charlesby. Viscosity relationship in solutions of polyethylene glycols. *Journal of Polymer Science*, **42**, 195–202, 1960.

[33] Michele S. McAfee, Huixiang Zhang, and Onofrio Annunziata. Amplification of salt-induced polymer diffusiophoresis by increasing salting-out strength. *Langmuir*, **30**, 12210–12219, 2014.

[34] R. J. Phillips. Gradient diffusion in dilute suspensions of hard spheroidal particles. *Journal of Fluid Mechanics*, **887**, A1–1–34, 2020.

[35] R. J. Ellis and A. P. Minton. Join the crowd. *Nature*, **425**, 27–28, 2003.

[36] M. S. McAfee and O. Annunziata. Effect of particle size on salt-induced diffusiophoresis compared to Brownian mobility. *Langmuir*, **30**, 4916–4923, 2014.

[37] S. S. L. Peppin, J. A. W. Elliott, and M. G. Worster. Pressure and relative motion in colloidal suspensions. *Physics of Fluids*, **17**, 053301, 2005.

[38] J. F. Richardson and W. N. Zaki. Sedimentation and fluidisation. part 1. *Trans. Inst. Chem. Eng.*, **32**, 35–53, 1954.

[39] C. D. Shackelford. Laboratory testing for waste disposal – A review. *J. Contam. Hydrol.*, **7**, 177–217, 1991.

[40] A. Einstein. *Investigations on the theory of Brownian movement.* Dover, U.S.A., 1956.

[41] W. Sutherland. A dynamical theory of diffusion for non-electrolytes and the molecular mass of albumin. *The London, Edinburgh, and Dublin Philosophical Magazine and Journal of Science*, **9**, 781–785, 1905.

[42] Anish Tuteja, Michael E. Mackay, Suresh Narayanan, Subashini Asokan, and Michael S. Wong. Breakdown of the continuum Stokes-Einstein relation for nanoparticle diffusion. *Nano Letters*, **7**, 1276–1281, 2007.

[43] Jun Liu, Dapeng Cao, and Liqun Zhang. Molecular dynamics study on nanoparticle diffusion in polymer melts: A test of the Stokes-Einstein law. *The Journal of Physical Chemistry C*, **112**, 6653–6661, 2008.

[44] R. Holyst, A. Bielejewska, J. Szymański, A. Wilk, A. Patkowski, J. Gapiński, A. Żywociński, T. Kalwarczyk, E. Kalwarczyk, M. Tabaka, N. Ziębacz, and S. A. Wieczorek. Scaling form of viscosity at all length-scales in poly(ethylene glycol) solutions studied by fluorescence correlation spectroscopy and capillary electrophoresis. *Phys. Chem. Chem. Phys.*, **11**, 9025–9032, 2009.

[45] Tai-Hsi Fan, Jan K. G. Dhont, and Remco Tuinier. Motion of a sphere through a polymer solution. *Phys. Rev. E*, **75**, 011803, 2007.

[46] Karol Makuch, Robert Holyst, Tomasz Kalwarczyk, Piotr Garstecki, and John F. Brady. Diffusion and flow in complex liquids. *Soft Matter*, **16**, 114–124, 2020.

[47] T. Kalwarczyk, K. Sozanski, S. Jakiela, A. Wisniewska, E. Kalwarczyk, K. Kryszczuk, S. Hou, and R. Holyst. Length-scale dependent transport properties of colloidal and protein solutions for prediction of crystal nucleation rates. *Nanoscale*, **6**, 10340–10346, 2014.

[48] Gregory S. Ullmann, Kathleen Ullmann, Robert M. Lindner, and George D. J. Phillies. Probe diffusion of polystyrene latex spheres in polyethylene oxide-water. *The Journal of Physical Chemistry*, **89**, 692–700, 1985.

[49] H. Zhang and O. Annunziata. Macromolecular hydration compared with preferential hydration and their role on macromolecule-osmolyte coupled diffusion. *Phys. Chem. Chem. Phys.*, **11**, 8923–8932, 2009.

[50] R.B. Jones. Diffusion of tagged interacting spherically symmetric polymers. *Physica A: Statistical Mechanics and its Applications*, **97**, 113 – 126, 1979.

[51] Hiromi Yamakawa. Transport properties of polymer chains in dilute solution: Hydrodynamic interaction. *The Journal of Chemical Physics*, **53**, 436–443, 1970.

[52] James W. Swan and Gang Wang. Rapid calculation of hydrodynamic and transport properties in concentrated solutions of colloidal particles and macromolecules. *Physics of Fluids*, **28**, 011902, 2016.

[53] J. A. Cohen, R. Podgornik, P. L. Hansen, and V. A. Parsegian. A phenomenological one-parameter equation of state for osmotic pressures of PEG and other neutral flexible polymers in good solvents. *The Journal of Physical Chemistry B*, **113**, 3709–3714, 2009.

[54] J. Li, M. Turesson, C. A. Haglund, B. Cabane, and M. Skepo. Equation of state of PEG/PEO in good solvent. Comparison *between* a one-parameter EOS and experiments. *Polymer*, **80**, 205 – 213, 2015.

[55] Indermeet Kohli and Ashis Mukhopadhyay. Diffusion of nanoparticles in semidilute polymer solutions: Effect of different length scales. *Macromolecules*, **45**, 6143–6149, 2012.

[56] Johann Gaube, Andreas Pfennig, and Matthias Stumpf. Vapor-liquid equilibrium in binary and ternary aqueous solutions of poly(ethylene glycol) and dextran. *Journal of Chemical & Engineering Data*, **38**, 163–166, 1993.